Composite Structures 117 (2014) 267–273

Contents lists available at ScienceDirect

Composite Structures

journal homepage: www.elsevier.com/locate/compstruct

A *crack length control scheme* for solving nonlinear finite element equations in stable and unstable delamination propagation analysis

Federico Gasco *, Paolo Feraboli

Dept. of Aeronautics and Astronautics, University of Washington, Seattle, WA 98195, USA

ARTICLE INFO

Article history:
Available online 4 July 2014

Keywords:
Delamination
Damage mechanics
Finite element analysis (FEA)
Virtual crack closure technique

ABSTRACT

An automatic incremental solution algorithm for nonlinear static finite element analysis of delamination propagation problems is presented. This load–displacement–constraint method iterates in the load displacement space utilizing the Newton–Raphson method, allowing to trace out the complete equilibrium path. The procedure can calculate pre- and post-critical responses of bi-dimensional problems, ranging from stable delamination growth to structural collapse by unstable growth or delamination buckling with arbitrarily sharp snap-back instabilities. Benchmark solution examples of established composite materials structural problems illustrate the effectiveness of the method.

1. Introduction

It is common practice to simulate the automatic delamination propagation in fiber reinforced polymer composites using finite element analysis (FEA) with direct application of linear elastic fracture mechanics (LEFM). Propagation occurs by allowing two coincident crack tip nodes to separate, causing a sudden loss of adhesion and a finite delamination length increase, which coincides with one element length. The computation of the mode decomposed strain energy release rate (ERR) is performed with the virtual crack closure technique (VCCT) [1]. Single or multiple delamination advancements can be allowed within a solution increment. In the first case the increment size is cutback if the total ERR, G_T, exceeds its critical value, G_C, by more than a certain release tolerance r_{tol}. The ERR convergence criterion to be satisfied is

$$\frac{G_T}{G_C} \leqslant 1 + r_{tol} \tag{1}$$

If the condition is not satisfied, the computed equilibrium configuration is discarded and the solution restarts with an increment size cut down, whereas the delamination is propagated when

$$1 \leqslant \frac{G_T}{G_C} \leqslant 1 + r_{tol} \tag{2}$$

In the second case the delamination is propagated until relation (1) is satisfied, but equilibrium has to be satisfied at every finite advancement. Therefore, for both procedures, at least one iteration per finite advancement is needed in order to obtain a converged equilibrium configuration. Moreover, the force imbalance suddenly increases upon delamination advancement because of the deletion of large nodal forces at the crack tip. This discontinuity in the out-of-balance forces in so severe that a number of iterations is required to reduce the force residuals within the convergence threshold. Hence the total number of iterations increases exponentially with mesh density.

Assuming that the loading is dependent on a single intensity parameter λ that controls the magnitude of all the applied loads, which are therefore proportionally varying, the load–displacement characteristic of the structure, also known as the equilibrium path, presents itself as a curve in the $N+1$ dimensional space spanned by the N degrees of freedom and λ, Fig. 1. As the failure becomes more brittle, the softening branch of the curve tends to assume a positive slope. Such a catastrophic event tends to reproduce the failure predicted by the LEFM because the process zone and the slow crack growth are negligible before unstable crack propagation occurs. The critical point at which the fracture starts to propagate is therefore a singular point where two branches having distinct tangents intersect. Dimensional analysis showed that large and/or slender structures with low fracture toughness and high tensile strength are associated with brittle propagation [2]. Since composite laminates are slender structures with large in-plane strength but relatively low fracture toughness, delamination propagation is intimately connected with such singularities. Hence, even if the composite is a linear elastic material and no elastic instabilities occur, passing the critical point can result in snap-back or snap-through instability due to the global softening associated to

* Corresponding author.
E-mail address: gasco@uw.edu (F. Gasco).

http://dx.doi.org/10.1016/j.compstruct.2014.06.038
0263-8223/

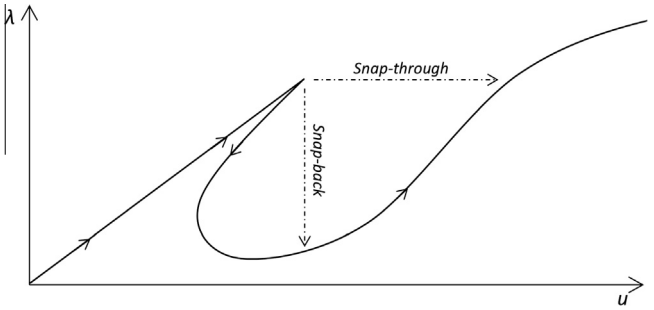

Fig. 1. Equilibrium path for a bi-dimensional case with snap-back or snap-through instability.

unstable delamination propagation, Fig. 1. When this occurs, a branch of the equilibrium path becomes virtual.

The implicit FEA method typically fails to converge upon unstable delamination propagation unless the structure is stabilized by adding artificial stiffness components [3]. This implies that a trial and error process is required to identify structural collapse and calculate the post collapse response. Repeated increment cutbacks are also necessary to reduce the increment size by several orders of magnitude in order to resolve the dynamic snapping, leading to a low computational efficiency. Moreover, the virtual branch remains unknown whereas tracing the full equilibrium path would allow to infer the structural response associated with different initial crack lengths without additional analysis.

In the analysis of elastic snap-through and snap-back instabilities, such as buckling of thin shells, load–displacement–constraint procedures [4] were successfully used to trace the full equilibrium path. These methods, known as arc-length methods, iterate in the load–displacement space using the Newton–Raphson (NR) method [5,6]. The increment Δl of the coordinate s that follows the path, Fig. 1, is employed as a solution control parameter. An auxiliary scalar equation constrains the norm of the incremental nodal displacements and the load factor λ to follow a spherical or cylindrical path with radius Δl. Therefore the applied load becomes an additional variable and it is not under user control. The parameter Δl controls the progress of the solution, thereby avoiding the high number of iterations and increment cutbacks while approaching the critical buckling load. However, in the analysis of elastic instabilities singular points present themselves in the form of saddle nodes, whereas it was documented that the arc-length method is not robust enough to resolve the sharp snap back instabilities associated with crack propagation [7,8]. In order to analyze this class of problems the arc-length method was modified by a number of authors, thereby becoming problem dependent. As a consequence, the method lost some of its generality and elegance. When the arc-length method was utilized in conjunction with the VCCT, the modification mentioned above was also necessary to cope with the spurious oscillations in the elastic response that are peculiar to the finite delamination propagation [7], the tangent stiffness matrix varying from positive definite to negative definite.

The objective of the method proposed hereinafter was to trace the full equilibrium path in a unified analysis and to increase the robustness and computational efficiency in the analysis of bi-dimensional delamination problems with the direct application of LEFM with VCCT.

2. The *crack length control scheme*

The proposed *crack length control scheme* (CLCS) consists in an automatic incremental solution algorithm for implicit nonlinear static finite element equations, designed to compute stable and unstable delamination propagation. Like the arc-length method, this load–displacement–constraint procedure iterates in the load–displacement space utilizing the NR method. The control parameter remains the coordinate s that follows the equilibrium path, and its linearized increment, the so called arc-length Δl. However, the constrained variables are not the load and the nodal displacements, but the load and the delamination length. In order to define a delamination length, the structural problem has to be idealized with a bi-dimensional model, such as plane strain, plane stress or axis-symmetric. The load intensity parameter λ can be defined, for example, as the magnitude of the applied loads resultant, p, divided by a normalizing force magnitude α

$$\lambda = \frac{p}{\alpha} \tag{3}$$

The analyst can arbitrarily select a nodal displacement variable u that identifies the nondimensional load–displacement space of interest. The load–displacement response is therefore defined in a bi-dimensional space $\lambda - u/\beta$, where β is a normalizing displacement magnitude, Fig. 2. Starting from a known equilibrium configuration at time t and using the notation in [4], the solution of the governing equations results in the following iterative scheme

$${}^{\tau}\boldsymbol{K}^{(i-1)}\Delta\boldsymbol{U}^{(i)} = {}^{t+\Delta t}\boldsymbol{R} - {}^{t+\Delta t}\boldsymbol{F}^{(i-1)} \tag{4}$$

where ${}^{\tau}\boldsymbol{K}^{(i-1)}$ is a tangent stiffness matrix, $\Delta\boldsymbol{U}^{(i)}$ is the correction at iteration i of the current displacement vector, ${}^{t+\Delta t}\boldsymbol{R}$ is the vector of externally applied nodal forces and ${}^{t+\Delta t}\boldsymbol{F}$ is the vector of nodal point forces equivalent to the internal element stresses, both being evaluated at time $t + \Delta t$. The system of N simultaneous equilibrium Eq. (4) is solved for $\Delta\boldsymbol{U}^{(i)}$ by splitting the increment Δt, identified by the arc $A - C$ in Fig. 2, into a growth sub-increment, $A - B$, which is solved first, and a subsequent equilibrium sub-increment, $B - C$, which computes the new equilibrium configuration ${}^{t+\Delta t}\boldsymbol{U}^{(i)}$. In terms of displacements

$${}^{t+\Delta t}_{g}\boldsymbol{U}^{({}_{g}i)} = {}^{t}_{g}\boldsymbol{U} + \boldsymbol{U}^{({}_{g}i)}, \quad \boldsymbol{U}^{({}_{g}i)} = \sum_{m=1}^{{}_{g}i}\Delta\boldsymbol{U}^{(m)} \tag{5}$$

$${}^{t+\Delta t}\boldsymbol{U}^{(i)} = {}^{t+\Delta t}_{g}\boldsymbol{U} + \boldsymbol{U}^{({}_{e}i)}, \quad \boldsymbol{U}^{({}_{e}i)} = \sum_{n=1}^{{}_{e}i}\Delta\boldsymbol{U}^{(n)} \tag{6}$$

$$i = {}_{g}i + {}_{e}i \tag{7}$$

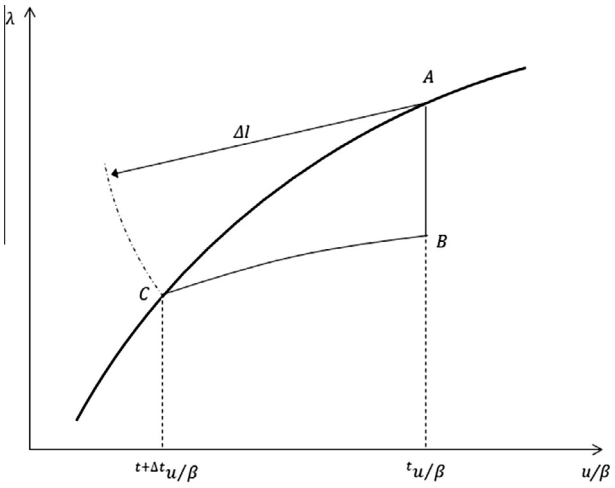

Fig. 2. Schematics of a *crack length control scheme* increment in a nondimensional load–displacement plot.

In the above equations the subscript g and e refer to the growth and equilibrium sub-increment.

Having a control parameter implies that the value of a set of variables, has to be constrained by an additional equation that includes the control parameter. The constrained variable of the growth sub-increment is the increment in delamination length Δa. The value of Δa is computed by solving a constraint equation as discussed below and the delamination is propagated through the number of finite elements that best approximates Δa at the beginning of the first iteration.

In order to solve the severe discontinuity of a finite propagation, full Newton–Raphson (FNR) iterations $({}_g i)$ are employed while the applied displacement is maintained constant, which is accomplished by performing the growth sub-increment under displacement control. The equilibrium equations to be solved are then

$$ {}^{t+\Delta t}_{g}\boldsymbol{K}^{({}_g i-1)}\Delta\boldsymbol{U}^{({}_g i)} = {}^{t+\Delta t}_{g}\boldsymbol{R}^{({}_g i)} - {}^{t+\Delta t}_{g}\boldsymbol{F}^{({}_g i-1)} \tag{8}$$

Maintaining the applied displacement constant allows to minimize the out-of-balance forces, thereby increasing the convergence rate. Alternatively constant loading can be employed in case of complex distributed loads.

The equilibrium sub-increment consists in converging to incipient growth under constant delamination length $a + \Delta a$. This is usually a relatively small load increment with mild geometric nonlinearities, which is solved with the FNR method or the BFGS method with line searches. The constrained variable of the equilibrium sub-increment is the applied load, which is controlled by scaling the applied load vector computed by the last converged iteration of the growth sub-increment. Scaling is performed by means of a load increment intensity parameter φ

$$ {}^{t+\Delta t}\widetilde{\boldsymbol{K}}^{({}_e i-1)}\Delta\boldsymbol{U}^{({}_e i)} = \varphi\ {}^{t+\Delta t}_{g}\boldsymbol{R} - {}^{t+\Delta t}\boldsymbol{F}^{({}_e i-1)} \tag{9}$$

The elastic branch of the equilibrium path is solved as an equilibrium sub-increment.

In order to develop the constraint equations that relate Δl to Δa and φ, let us consider a linearized structural response at the configuration at time t. An approximate relation between the delamination length increment ${}^{t+\Delta t}\Delta a$ and the arc-length that spans from t to $t + \Delta t$ is derived from an explicit computation of the load and displacement components of Δl using the forward Euler method, Fig. 3. The time variable associated with this linearly extrapolated response is indicated as $t + \Delta\tilde{t}$ to remark that it is an approximate estimation. The length ${}^{t+\Delta t}\Delta a$ is indicated as Δa for clarity. By introducing the compliance C, which refers to the load p and the displacement u, and expanding the components of the arc-length with Taylor series we obtain

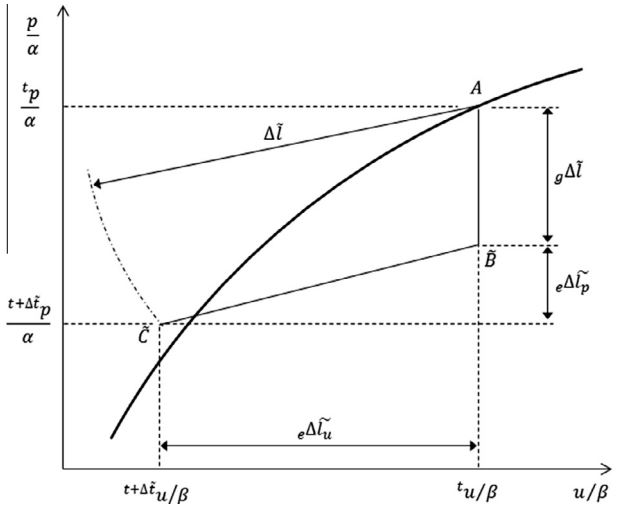

Fig. 3. Linear extrapolation of the arc-length components.

$$ {}_g\Delta\tilde{l} = \frac{1}{\alpha}\,{}^t\left(\frac{dp}{da}\right)_u \Delta a \tag{10}$$

$$ {}_e\Delta\tilde{l}_p = \frac{\varphi-1}{\alpha}\left[{}^t\left(\frac{dp}{da}\right)_u \Delta a + {}^t p\right] \tag{11}$$

$$ {}_e\Delta\tilde{l}_u = \frac{\varphi-1}{\beta}\left[{}^tC\,{}^t\left(\frac{dp}{da}\right)_u \Delta a + {}^tC\,{}^t p + {}^t\left(\frac{dC}{da}\right)\Delta a\,{}^t p + {}^t\left(\frac{dC}{da}\right){}^t\left(\frac{dp}{da}\right)_u \Delta a^2\right] \tag{12}$$

Eq. (12) is simplified by neglecting the last member of the addition, which gives

$$ {}_e\Delta\tilde{l}_u \cong \frac{\varphi-1}{\beta}\left\{\left[{}^tC\,{}^t\left(\frac{dp}{da}\right)_u + {}^t\left(\frac{dC}{da}\right){}^t p\right]\Delta a + {}^tC\,{}^t p\right\} \tag{13}$$

The first constraint equation is obtained by substituting Eqs. (10), (11), and (13) into the following arc-length condition

$$ \left({}_g\Delta\tilde{l} + {}_e\Delta\tilde{l}_p\right)^2 + {}_e\Delta\tilde{l}_u{}^2 = \Delta l^2 \tag{14}$$

Eq. (14) is a quadratic equation in the unknown Δa and can be written as

$$ X\Delta a^2 + \Psi\Delta a + \Omega = 0 \tag{15}$$

where

$$ X = \frac{\varphi^2}{\alpha^2}\,{}^t\left(\frac{dp}{da}\right)_u^2 + \frac{(\varphi-1)^2}{\beta^2}\left[{}^tC\,{}^t\left(\frac{dp}{da}\right)_u + {}^t\left(\frac{dC}{da}\right){}^t p\right]^2 \tag{16}$$

$$ \Psi = \frac{2(\varphi^2-\varphi)}{\alpha^2}\,{}^t\left(\frac{dp}{da}\right)_u {}^t p + \frac{2(\varphi-1)^2}{\beta^2}\left[{}^tC^2\,{}^t p\,{}^t\left(\frac{dp}{da}\right)_u + {}^tC\,{}^t p^2\,{}^t\left(\frac{dC}{da}\right)\right] \tag{17}$$

$$ \Omega = (\varphi-1)^2\left[\frac{1}{\alpha^2}\,{}^t p^2 + \frac{1}{\beta^2}\,{}^tC^2\,{}^t p^2\right] - \Delta l^2 \tag{18}$$

Eq. (15) is solved at the beginning of each growth sub-increment in order to update the delamination length for a given Δl. A root of the equation is positive, which corresponds to the delamination length increment that allows the solution to proceed forward along the equilibrium path. The other root is negative, which corresponds to the opposite path direction. Since a is monotonically increasing with time, always the positive root should be selected. In order to solve Eq. (15), however, the values of the derivatives of the load and the compliance with respect to the crack length and the value of the load increment intensity parameter φ have to be determined. The two derivatives can be computed by backward difference or analytic models. The results presented in the next section were obtained with analytic sensitivity. The description of the numerical computation of the derivative by backward difference is omitted. The analytic relation between the variation of compliance and strain energy upon infinitesimal delamination propagation can be found by applying the Castigliano's theorem to a generic linear elastic body with a crack and an applied load p. This relation substituted into the definition of strain energy release rate gives the following analytic sensitivity equation [9]

$$ {}^t\left(\frac{dC}{da}\right) = \frac{2b\,{}^tG_T}{{}^t p^2} \tag{19}$$

where b is the width of the bi-dimensional structural problem under consideration. For a displacement controlled structure, with a similar derivation, we obtain [9]

Table 1
User inputs for the *crack length control scheme*.

	Δa_0 [mm]	Δa_{min} [mm]	Δa_{max} [mm]	α [N^{-1}]	β [mm^{-1}]	c_{tol} [–]	n_d [–]
SLB	5	1	10	1	0.018	0.005	12
DCB	1	1	2.5	1	0.0374	0.005	12
Delamination buckling	2	2	5	1000	0.002	0.01	12

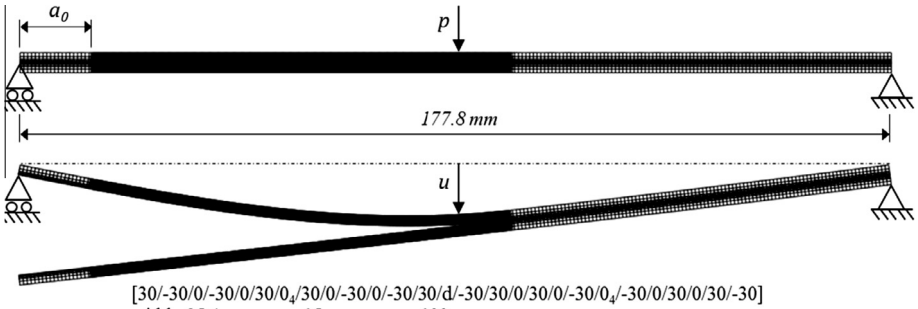

Fig. 4. FEM of SLB specimen at zero and maximum unscaled deformation. Mesh size adjacent to delaminated interface 0.125 mm.

$$ {}^{t}\left(\frac{dp}{da}\right)_u = -\frac{2b\,{}^{t}G_T}{{}^{t}u} \tag{20}$$

Although more elegant than the numerical sensitivity, the analytical sensitivity is less general because, as a condition for the application of the Castigliano's theorem, the displacement u must be the displacement at the point of application of the force p in the direction of p.

The parameter φ can be approximated by the ratio of the extrapolated load at the end of the increment, ${}^{t+\Delta t}p$, to the one at the end of the growth sub-increment, ${}^{t+\Delta t}_{g}p$,

$$\tilde{\varphi} = \frac{{}^{t+\Delta t}p}{{}^{t+\Delta t}_{g}p} \tag{21}$$

By substituting Eq. (20) into (22) and noting that, for small increments, the derivative of the compliance with respect to the crack length can be considered constant throughout an equilibrium sub-increment, we obtain that at incipient delamination growth

$$\tilde{\varphi} = \left(\frac{{}^{t}G_C}{{}^{t+\Delta t}_{g}G_T}\right)^{1/2} \tag{22}$$

In the above equation the mode mixity is assumed constant between two consecutive increments. The error associated with this assumption can be expected to be small provided that elastic instabilities do not occur and that the delamination length increments are small enough. The strain energy release rate ${}^{t+\Delta t}_{g}G_T$ is computed with the following second order numerical method

$$ {}^{t+\Delta t}_{g}G_T = {}^{t}G_T + {}^{t}\left(\frac{dG_T}{da}\right)_u \Delta a + \frac{1}{2}\frac{{}^{t}\left(\frac{dG_T}{da}\right)_u - {}^{t-\Delta t}\left(\frac{dG_T}{da}\right)_u}{{}^{t}\Delta a}\Delta a^2 \tag{23}$$

The derivatives of the energy release rate were computed with backward difference between the end and the beginning of the preceding growth sub-increment.

The system of two coupled constraint Eqs. (15) and (23) is solved by numerical iterations, starting from an initial numerical value for Δa equal to ${}^{t}\Delta a$. The range of allowable values of Δa is limited by a maximum and minimum value Δa_{min} and Δa_{max}. This provides the finite delamination length increase to be applied in the current increment, whereas φ is calculated from Eq. (23) at the beginning of each equilibrium sub-increment using the ERR computed at the end of the growth sub-increment. A small perturbation increment is applied at the beginning of the analysis in order to compute the ERR required by the subsequent equilibrium sub-increment. Once the solution is converged at the critical point, the delamination is propagated within the first growth sub-increment by a user defined amount Δa_0.

The arc-length update, which is controlled by the convergence rate, is performed as follows

$$\Delta l_{new} = \sqrt{\frac{n_d}{n_t}}\Delta l_{old} \tag{24}$$

where n_d is the desired number of iterations per increment and n_t is the total number of iterations of the previous increment.

The solution of a growth sub-increment is initially attempted in one step. However, if either the force or the displacement convergence criterion is not satisfied within 16 iterations, Δa is

Table 2
Unidirectional material data.

	E_1 [GPa]	$E_2 = E_3$ [GPa]	$G_{12} = G_{13}$ [GPa]	G_{23} [GPa]	$\nu_{12} = \nu_{13} = \nu_{23}$	G_{IC} [MPa]	G_{IIC} [MPa]	η[a]	Ply thickness [mm]
Material 1	146.86	10.62	5.45	3.99	0.33	248[b]	865[b]	1.512[c]	0.127
Material 2	162	8.34	4.96	3.11	0.34	316	579	1.6	0.127

[a] Exponent of BK law.
[b] Mean values of precracked specimens [11].
[c] Calculated based on mode mix ratio reported in [12].

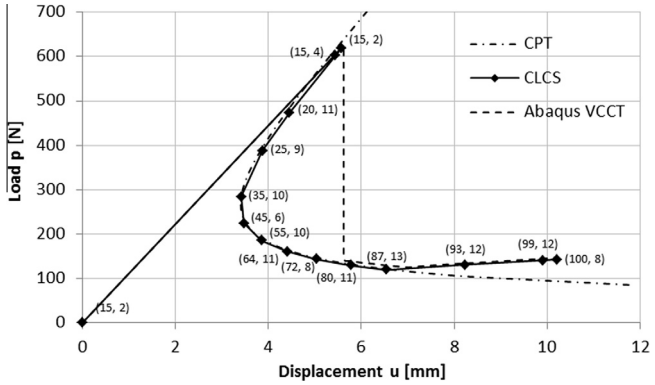

Fig. 5. *Crack length control scheme* (CLCS), Abaqus VCCT and closed form (CPT) solutions of SLB test. Curve markers indicate converged increments. The delamination length [mm] and the total number of iterations required to converge are indicated in parenthesis.

progressively cut down automatically. Equilibrium sub-increments must satisfy the same convergence criteria mentioned above, which ensure that the equilibrium is satisfied, but they also must satisfy the following additional ERR criteria

$$\left|\frac{{}^{t+\Delta t}G_T^{(i)}}{{}^{t+\Delta t}G_C^{(i)}} - 1\right| \leqslant c_{tol} \tag{25}$$

which ensures convergence to incipient delamination growth. If either the force or the displacement condition is not satisfied, the sub-increment is then reattempted through multiple FNR increments. The automatic increment control scheme consists in cutting down the equilibrium sub-increment size into 10 reduced increments of equal size. If necessary, the size is further reduced to obtain 100 reduced increments. If the force and displacement criteria are satisfied, the solution is accepted because an equilibrium configuration has been found. However, if the ERR criterion has been overshoot, the equilibrium sub-increment restarts from the new configuration with the increment size cut down described above. When the increment cut down process is activated, the solution always restarts form the last iteration that satisfied the force and displacement convergence criteria. Moreover, φ is updated at the beginning of each increment. A peculiar characteristic of the CLCS is that at any iteration an equilibrium sub-increment is declared converged when all three convergence criteria are satisfied. This feature, together with the increment size cut down, avoids solution oscillations with repeated overshooting of the ERR convergence condition. If the reduction of the increment size is not successful in achieving convergence, artificial stabilization techniques are automatically applied for either growth or equilibrium sub-increments. The physical meaning and numerical repercussions of the convergence tolerance c_{tol} on the accuracy of the solution are the same as the release tolerance r_{tol}. For both of them, if the convergence tolerance is too large inaccurate results are obtained, whereas if the tolerance is too tight much computational effort is spent to obtain needless accuracy. The remarkable difference is that in a conventional VCCT implementation a converged equilibrium configuration is discarded if the ERR convergence criteria is not satisfied, Eq. (1), whereas the CLCS uses that converged equilibrium as a restart configuration. Among the input parameters that were mentioned in this section, seven are peculiar to the CLCS, Table 1, whereas the others are required by any nonlinear analysis.

The proposed method can be applied to cohesive zone modeling (CZM), provided that the ERR convergence criteria, Eq. (25), is replaced by the incipient delamination growth condition specified by the traction–separation law.

3. Benchmarks

The CLCS was implemented in Abaqus/Standard by means of a Python script that called a restart job for each sub-increment. Simulation of a single leg bending test (SLB), a double cantilever beam test (DCB) and a delamination buckling problem were conducted to assess the effectiveness of the method in case of unstable delamination propagation, stable propagation and elastic instability respectively. The performance of the proposed method was compared to established closed form and the Abaqus VCCT solutions. All the Abaqus VCCT solutions were obtained in a single FNR step, with an initial increment size of 0.001 and a maximum increment size of 0.25. The increment size was automatically controlled based on the default Abaqus increment control scheme settings [10], except for the maximum number of solution attempts which was increased to 100 to resolve unstable propagation. The tolerance r_{tol} was set to 0.1. The settings for the CLCS are listed in Table 1.

Existing experimental data, closed form solutions and numerical simulations for the material and specimen configuration adopted for the SLB test can be found in [11,12], Fig. 4. The material was named 'material 1' and its properties are listed in Table 2. The result obtained with the CLCS method is shown in Fig. 5. The curve markers indicate the system configurations at the end of each converged equilibrium sub-increments. The load–displacement curve was in good agreement with the prediction of the classical plate theory (CPT) analytic solution [13]. All the increments converged without cutting down the delamination length increment (growth) or the load increment (equilibrium). Convergence to incipient growth was always successful at the first attempt, except for the elastic branch where the linear analytic model that was utilized

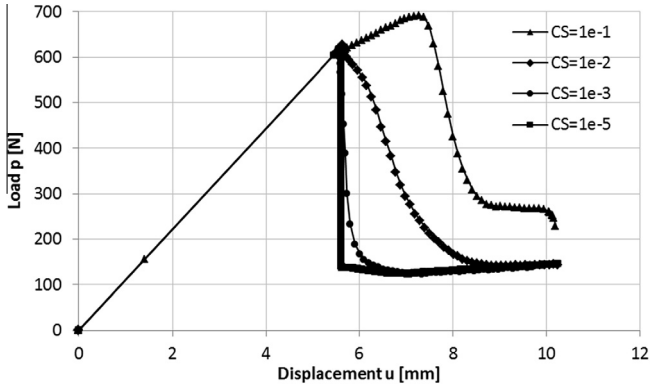

Fig. 6. Convergence study for contact stabilization coefficient (CS).

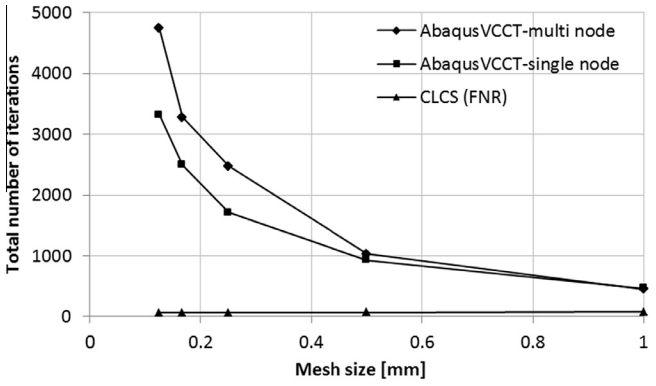

Fig. 7. Total number of iterations vs. mesh size at delaminated interface.

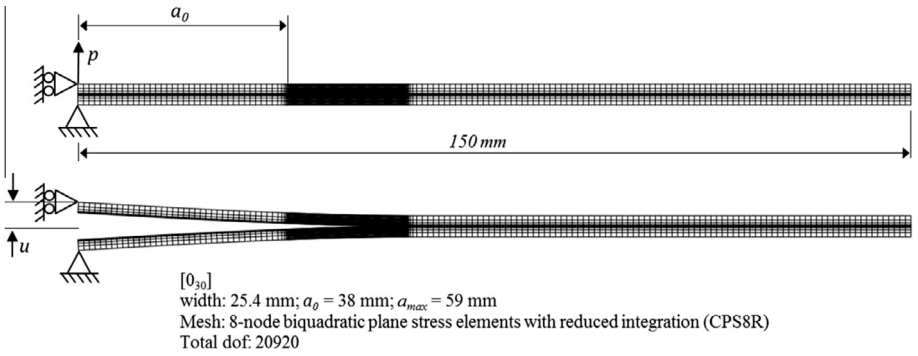

Fig. 8. FEM of DCB specimen at zero and maximum unscaled deformation. Mesh size 0.125 mm along the delaminated interface.

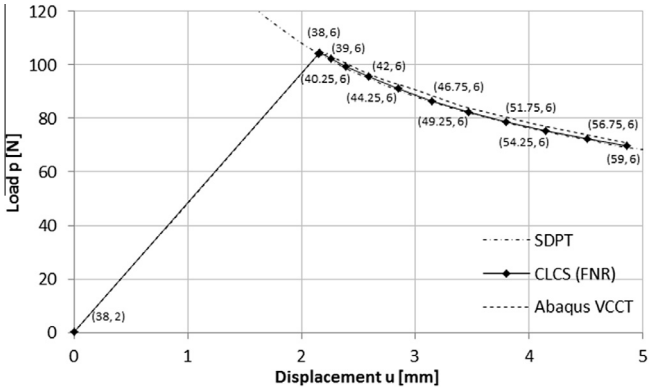

Fig. 9. *Crack length control scheme* (CLCS), Abaqus VCCT and closed form (SDPT) solutions. Curve markers indicate converged increments. The delamination length and the number of iterations required to converge are indicated in parenthesis.

to compute φ underestimated the critical load because of geometric nonlinearities. For the same finite element discretization the Abaqus VCCT solution cut down the increment size by seven orders of magnitude in order to capture the sharp load drop and it required contact stabilization, a stabilization technique based on localized artificial nodal stiffness at the opening delamination surfaces [10]. The stabilization coefficient was determined through a convergence study. The results shown in Fig. 6 confirm that, when the structural response is unknown a priori, the unstable propagation could remain undetected and the critical load be overestimated if an appropriate convergence study is not performed [3]. On the other hand, the CLCS did not require artificial stabilization because the applied displacement is fixed during growth. The number of Abaqus VCCT iterations increased exponentially as the mesh size at the delaminated interface was reduced, whereas the CLCS iterations were almost independent from the mesh size and one or two orders of magnitude smaller, Fig. 7. The solution time of the BFGS method was on average 65% higher than FNR for a number of degrees of freedom ranging from 10 to 64 k.

The structural response of an arbitrary DCB specimen made of 'material 2', Fig. 8, was calculated with the CLCS, the Abaqus VCCT and the closed form solution based on the shear deformable plate theory (SDPT) [14]. The results of the three analysis methods were in good agreement, Fig. 9. Similar to the SLB example, all the increments converged at the first attempt, except for the large increment that traced the elastic branch. In total 68 FNR iterations were necessary for the CLCS to solve the problem, whereas the Abaqus VCCT solution required 856 iterations for the single advancement method and 805 iterations for the multiple advancements method. The BFGS method was as computationally efficient as the FNR method in solving equilibrium sub-increments, taking about the same average CPU time per increment.

The simultaneous occurrence of unstable delamination propagation and elastic instability was reproduced by means of a delaminated plate loaded under uniaxial compression, Fig. 10. The material was 'material 2' with degraded G_{IC} and G_{IIC} to 189 and 347 J/m^2, respectively. The load was applied at the mid-depth of the lower sub-laminate. The computed response is plotted in Fig. 11. The size of the first four equilibrium sub-increments on the softening branch, indicated with hollow markers, was automatically cut down by the CLCS. The reason was the overshoot of the ERR convergence criterion. Also the increments E to H failed the ERR convergence condition, but G_T did not exceeded G_C. In this case the increment was automatically simply restarted with an

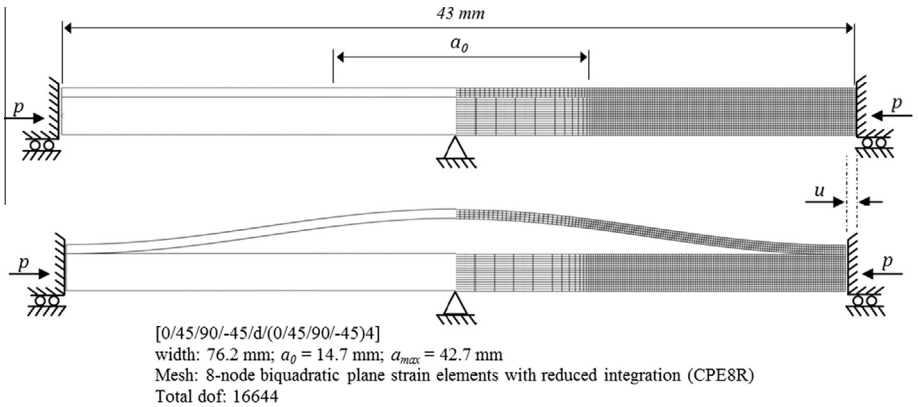

Fig. 10. FEM of delamination buckling specimen at zero and maximum unscaled deformation. Mesh size adjacent to delaminated interface 0.125 mm.

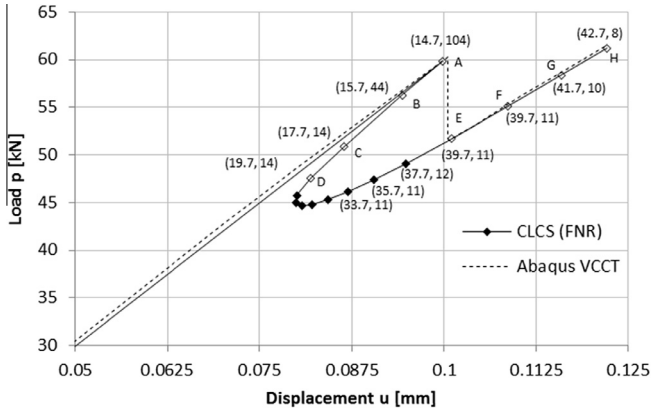

Fig. 11. *Crack length control scheme* (CLCS) and Abaqus VCCT solutions of delamination buckling. Curve markers indicate converged configurations. The delamination length and the number of iterations required to converge are indicated in parenthesis.

updated φ value as described in the previous section. All the growth sub-increments converged at the first attempt. Furthermore, the CLCS did not require the use of contact stabilization unlike the Abaqus VCCT solution. The solution of the constraint equations provided large values of Δa, that largely exceeded the specified Δa_{max}. The reason was the nonlinear structural response caused by the elastic instability. The use of analytic sensitivity to compute the load and compliance derivatives led to particularly large errors because of the combined effect of assuming linear elastic structural response and of the linearization performed by the forward Euler method. The numeric sensitivity performed slightly better, but the computed values for Δa were still affected by a too large error to be utilized in the arc-length control. Also the abrupt change in the delamination mode mixity caused by the local buckling contributed to the arc-length control failure. To cope with the nonlinear response, the algorithm was modified so that a constant delamination length increment, equal to Δa_{min}, was prudentially used if the computed valued of Δa was larger than $2\Delta a_{max}$ or in case of numerical divergence in the solution of the constraint equations. Nevertheless the CLCS required 293 FNR iterations to solve the problem, compared to the 1698 iterations of the Abaqus VCCT with a single advancement per increment and the 612 iterations with multiple advancements per increment. The BFGS method showed about the same computational efficiency of the FNR method.

4. Conclusions

Although it does not guarantee convergence, the CLCS method showed improved convergence rate and robustness with respect to the conventional VCCT implementation in tracing the complete equilibrium path of the structure with continuation through singular points. The enhanced computational efficiency was attributed to three reasons. The first was the capability of advancing the delamination by multiple element lengths. The second consisted in controlling the load increment size by means of the energy release rate, thereby avoiding unduly expensive load cutbacks. The last was the automatic selection of the largest increment size that ensured the computation of the structural response with the desired resolution. The use of the delamination length as a constrained variable, instead of the nodal displacements used by the arc-length method, led to an improved robustness. In fact, since the delamination length is monotonically increasing with time, the algorithm never fails in selecting the correct equilibrium path direction, even in presence of arbitrarily sharp singularities in the structural response. The drawback of the CLCS consists in the dependency of the constraint equation and convergence criteria to the delamination topology, i.e. to the element connectivity. As a result, the delamination has to be tracked constantly during the solution process, leading to a cumbersome addition to a finite element code. This requirement seems to be the main limitation for the extension of the method to the solution of three-dimensional problems.

References

[1] Rybicki EF, Kanninen MF. A finite element calculation of stress intensity factors by a modified crack closure integral. Eng Fract Mech 1977;9:931–8.
[2] Carpinteri A. Softening and snap-back instability in cohesive solids. Int J Numer Meth Eng 1989;28:1521–37.
[3] Krueger R. An approach for assessing delamination propagation capabilities in commercial FE codes. In: Proceedings of the ASC 22nd Technical Conference, Seattle, WA; 2007.
[4] Bathe KJ. Finite element procedures. Englewood Cliffs, NJ: Prentice Hall; 1996.
[5] Riks E. An incremental approach to the solution of snapping and buckling problems. Int J Solids Struct 1979;15:529–51.
[6] Crisfield MA. A fast incremental/iterative solution procedure that handles snap-through. Comput Struct 1981;13:55–62.
[7] Alfano G, Crisfield MA. Finite element interface models for the delamination analysis of laminated composites: mechanical and computational issues. Int J Numer Meth Eng 2001;50:1701–36.
[8] Hellweg HB, Crisfield MA. A new arc-length method for handling sharp snap-backs. Comput Struct 1998;66(5):705–9.
[9] Anderson TL. Fracture mechanics – Fundamentals and applications. 3rd ed. Boca Raton, FL: CRC Press, Taylor & Francis Group; 2005.
[10] Abaqus 6.12 User's Manual.
[11] Polaha JJ, Davidson B, Hudson RC, Pieracci A. Effects of mode ratio, ply orientation and precracking on the delamination toughness of a laminated graphite/epoxy composite. J Reinf Plast Compos 1996;15(2):141–73.
[12] Davidson BD, Krueger R, Konig M. Three-dimensional analysis of center-delaminated unidirectional and multidirectional SLB specimens. Compos Sci Technol 1995;54:385–94.
[13] Davidson BD, Sundararaman V. A single leg bending test for interfacial fracture toughness determination. Int J Fract 1996;78:193–210.
[14] O'Brien TK, Martin RH. Results of ASTM round robin testing for mode I interlaminar fracture toughness of composite materials. J Compos Tech Res 1993;15(4):269–81.